Carbon Dots

International Edition: DOI: 10.1002/anie.201501912
German Edition: DOI: 10.1002/ange.201501912

Cu–N Dopants Boost Electron Transfer and Photooxidation Reactions of Carbon Dots**

Wenting Wu, Liying Zhan, Weiyu Fan, Jizhong Song, Xiaoming Li, Zhongtao Li, Ruiqin Wang, Jinqiang Zhang, Jingtang Zheng, Mingbo Wu, and Haibo Zeng**

Abstract: *The broadband light-absorption ability of carbon dots (CDs) has inspired their application in photocatalysis, however this has been impeded by poor electron transfer inside the CDs. Herein, we report the preparation of Cu–N-doped CDs (Cu-CDs) and investigate both the doping-promoted electron transfer and the performance of the CDs in photooxidation reactions. The Cu–N doping was achieved through a one-step pyrolytic synthesis of CDs with Na_2[Cu(EDTA)] as precursor. As confirmed by ESR, FTIR, and X-ray photoelectron spectroscopies, the Cu species chelates with the carbon matrix through Cu–N complexes. As a result of the Cu–N doping, the electron-accepting and -donating abilities were enhanced 2.5 and 1.5 times, and the electric conductivity was also increased to 171.8 $\mu s\,cm^{-1}$. As a result of these enhanced properties, the photocatalytic efficiency of CDs in the photooxidation reaction of 1,4-dihydro-2,6-dimethylpyridine-3,5-dicarboxylate is improved 3.5-fold after CD doping.*

Increasing interest in photooxidation has been fueled by the ecological and economical advantages of using visible light as an abundant source of energy. For the efficient conversion of light energy into chemical energy and in related areas, photocatalytically active nanomaterials have been employed as photocatalysts to study electron-transfer processes and in charge separation.[1] The challenge in this area is to develop more low-cost photocatalysts to replace the known limited photocatalysts based on noble-metal nanoparticles, such as Ru nanoparticles.[1b] Fortunately, carbon dots (CDs) shows unique electron transfer and broadband light-absorbing abilities, a large specific surface area, and are abundant, inexpensive, and nontoxic.[2–13] These excellent properties are beneficial to intermolecular electron transfer, which plays a key role in many photooxidation reactions. However, most of the recent research has focused mainly on the emission properties of CDs.[5,6,10–12] There have been few recent efforts devoted to the fabrication of composites based on CDs to enhance their photocatalytic ability.[4,14–16] For example, Kang et al. prepared Au/CD composites as photocatalysts for the oxidation of cyclohexane in the presence of H_2O_2.[14] CD/TiO_2 nanotube composites were prepared for the degradation of rhodamine B.[17,18] However, CDs alone as photocatalysts show great potential. There have been relatively few examples of unfunctionalized CDs employed as photocatalysts which were designed to have enhanced electron-transfer properties, such as an electron-accepting ability, electron-donating ability, and conductivity.[4,19]

The selection of functionalized precursors with a fixed structure is a powerful approach to the design of novel CDs. Ethylenediaminetetraacetic acid (EDTA), with a flexible structure, is a common starting material for CDs. Interestingly, a saturated Schiff-base-like structure could be formed after EDTA chelated with metal ions such as Cu^{II} (Na_2[Cu(EDTA)]). Using Cu^{II} complexes, which prefer square-planar geometries,[20] a flaky graphite conductive structure could be easily formed. Cu complexes themselves used as commercial photocatalysts play important roles in electron-transfer processes for the conversion of solar energy.[20–23] For example, incorporating Cu complexes with the Schiff base ligand into zeolite significantly enhanced the photocatalytic ability.[20] Therefore, Na_2[Cu(EDTA)] is a new source with an saturated Schiff-base-like planar structure to fabricate novel CDs.

Herein, Cu–N-doped CDs (Cu-CDs) were prepared by a facile one-step pyrolytic synthesis from Na_2[Cu(EDTA)] precursors. During pyrolysis, this saturated Schiff-base-like structure transforms into a Cu coordination complex chelated with graphene matrixes, which is confirmed by ESR, TEM, XRD, FTIR, Raman, and X-ray photoelectron (XPS) spectroscopies. Under an atmosphere of air instead of pure oxygen, Cu-CDs were used as the photocatalyst for the photooxidation reaction of 1,4-dihydro-2,6-dimethylpyridine-3,5-dicarboxylate (1,4-DHP), which is the key component in a variety of bioactive compounds, such as anti-hypertensives and calcium-channel blockers.[24] This Cu-CD material, unlike previous CD-based composite photocatalysts, show outstanding electron-transfer properties. The conversion of 1,4-DHP

[*] W. T. Wu, L. Y. Zhan, W. Y. Fan, Z. T. Li, R. Q. Wang, J. Q. Zhang, J. T. Zheng, M. B. Wu
State Key Laboratory of Heavy Oil Processing
School of Chemical Engineering, China University of Petroleum
Qingdao 266580 (China)
E-mail: wumb@upc.edu.cn
W. T. Wu, J. Z. Song, X. M. Li, Prof. Dr. H. Zeng
Institute of Optoelectronics and Nanomaterials
Herbert Gleiter Institute of Nanoscience
School of Materials Science and Engineering
Nanjing University of Science and Technology
Nanjing, 210094 (P.R. China)
E-mail: zeng.haibo@njust.edu.cn

[**] This work was financially supported by the National Basic Research Program of China (2014CB931700), NSFC (61222403, 21302224, 20876176, 51303212, 51372277, 51172285, and 51303202), China Postdoctoral Science Foundation (2014M560590), Shandong Provincial Natural Science Foundation (ZR2013BQ028 and ZR2013EMQ013), Project of Science and Technology Program for Basic Research of Qingdao (14-2-4-47-jch) and the State Key Laboratory of Fine Chemicals (KF1203).

Supporting information for this article is available on the WWW under http://dx.doi.org/10.1002/anie.201501912.

catalyzed by Cu-CDs is 3.5 times higher than that of CDs without Cu–N doping.

Cu-CDs were prepared through thermolysis of Na_2[Cu(EDTA)] at 250 °C, 300 °C, and 350 °C, as shown in Figure 1 a. When the temperature is lower than 250 °C, it is hard to carbonize Na_2[Cu(EDTA)] to form CDs. On the other hand, when the temperature is higher than 350 °C, the carbonization degree is too high to form CDs in the nanoscale, resulting instead in the formation of powders on the microscale. An atomic absorption spectrum verified that the Cu content in

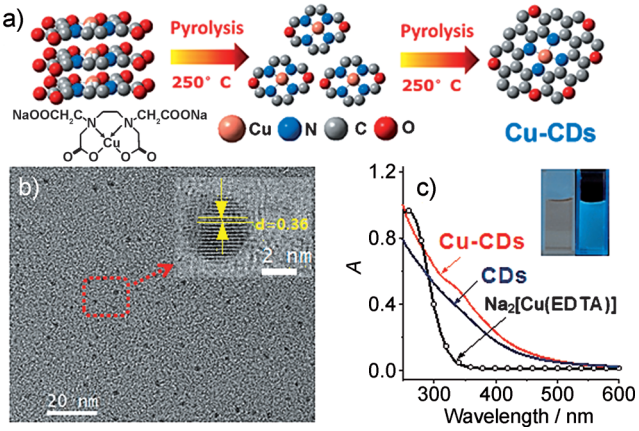

Figure 1. a) Schematic representation of the pyrolytic synthetic procedure for Cu-CDs. b) TEM and HRTEM (inset) images of Cu-CDs. c) UV/Vis absorption spectra of Cu-CDs, compared with CDs and Na_2[Cu(EDTA)] precursors. Inset in (c): photographs showing Cu-CDs in daylight (left) and under UV-light irradiation ($\lambda = 365$ nm).

Significantly, the visible-light-harvesting ability of CDs was greatly enhanced after doping, as shown in Figure 1 c. Na_2[Cu(EDTA)] absorbs strongly only in the UV region of the electromagnetic spectrum. However, Cu-CDs show a broadband absorption from $\lambda = 300$ nm to 600 nm. Meanwhile, the absorption intensity of Cu-CDs is higher than that of pure CDs, which could be attributed to the existence of Cu–N dopants, producing Cu-to-graphite charge-transfer (CT) absorption.[30,31] The color of the Cu-CD solution is brown, as shown in the inset of Figure 1 c. The solution of Cu-CDs gives blue emission upon excitation by UV light at $\lambda = 365$ nm. After irradiation for 160 min, there is no obvious photobleaching for Cu-CDs, indicating that Cu-CDs are stable (Figure S5), which will be beneficial for their application in photocatalysis.

The valence states of the Cu species in Cu-CDs were further investigated, as shown in Figure 2 and Figure S7. The high-resolution Cu 2p XPS spectra (Figure S7) shows the presence of Cu in Cu-CDs (932.5 eV, 934.2 eV, 952.5 eV).[32–34]

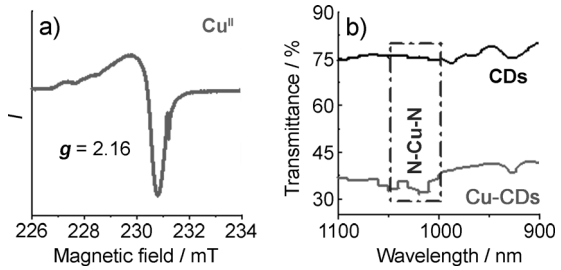

Figure 2. a) ESR spectrum of Cu^{II} in Cu-CDs. b) Amplified FTIR spectra of Cu-CDs and CDs.

CDs decreased with increasing temperature (see Figure S1 in the Supporting Information). For Cu-CDs prepared at 250 °C, denoted Cu-CDs(250), the Cu content is 2.1 %. However, as temperatures were increased to 300 °C and 350 °C, the Cu content decreased to 1.0 % and 0.59 %, respectively. This may be as a result of the easier reduction of Cu^{II} by carbon at higher temperature, which is confirmed by the XRD results. The XRD pattern of the precipitate after centrifugation of the mixture containing Cu-CDs(250) shows prominent peaks at 26° (graphite carbon), 43° (Cu^0), and 50°(Cu^0) (Figure S2a).[25,26] However, the precipitate prepared at 350 °C (Figure S2b) shows a weaker peak attributable to graphite at 26°. These results indicate that Cu^{II} was easily reduced into Cu^0 by carbon, and the higher thermolysis temperature causes the decrease of Cu^{II} content in Cu-CDs. In this work, Cu-CDs were prepared at 250 °C.

The TEM image of Cu-CDs clearly displays the uniformity of Cu-CDs with an average diameter of about 2.3 nm, as shown in Figure 1 b and Figure S3. The high-resolution TEM (HRTEM) image demonstrates the good crystallinity of Cu-CDs with a lattice spacing of 0.36 nm corresponding to the lattice fringes of the (002) planes of graphite.[27] The XRD and Raman spectroscopic results were consistent with these results (Figure S4), supporting the formation of a graphite-like structure,[1,18,28,29] which should be beneficial for enhancing conductivity in the electron-transfer process.

Therefore, it demonstrates the existence of Cu^{II} in Cu-CDs prepared by the one-step pyrolytic synthesis. To further analyze the valence state of copper, Cu-CDs were measured by ESR spectroscopy at room temperature, as shown in Figure 2 a. If the g tensor parameter (g) is less than 2.3, the species can be assigned to being in a covalent environment, otherwise it is in an ionic environment. The g value of Cu-CDs is 2.16, which is less than 2.3, indicating the covalent character of the Cu^{II}–ligand bond inside CDs.[35] The FTIR spectra of Cu-CDs from 900 to 1100 cm^{-1} were amplified to further characterize the chemical bond between the Cu and the matrix, as shown in Figure 2 b and Figure S8. Compared with pure CDs, Cu-CDs show new bands at 1050 cm^{-1} and 1020 cm^{-1}, which can be assigned to a N-Cu-N stretching vibration, further confirming the formation of Cu coordination complexes in Cu-CDs.[36]

To compare the photocatalytic abilities of Cu-CDs with pure CDs, the photooxidation of 1,4-DHP was carried out as shown in Figure 3 a and Figure S9. 1,4-DHP was irradiated under an atmosphere of air instead of an atmosphere of pure oxygen. Upon irradiation of the mixed solution of Cu-CDs and 1,4-DHP with a xenon lamp ($\lambda_{ex} > 385$ nm; Figure 3b), the absorption of 1,4-DHP at $\lambda = 374$ nm decreased and the absorption of the product (pyridine derivatives, **1b** in Figure 3a) at $\lambda = 280$ nm increased. The formation of the

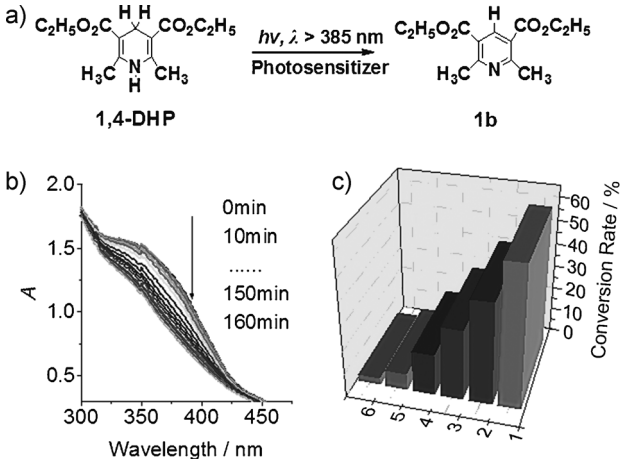

Figure 3. a) The photooxidation of 1,4-DHP to form product **1b**. b) UV/Vis absorption spectral evolution during photooxidation of DHP (1.0×10^{-4} M) in H_2O/ethanol ($v/v=1:1$) (c(Cu-CDs) = 0.15 mg mL^{-1}, 20 °C). This mixed aqueous solution was irradiated by a 35 W Xenon lamp (600 W·m^{-2}, $\lambda_{ex}>385$ nm). c) The conversion rate of 1,4-DHP catalyzed by Cu-CDs prepared at different thermolysis temperatures or using other photocatalysts: 1) Cu-CDs(250), 2) Cu-CDs(300), 3) Cu-CDs(350), 4) CDs, 5) no sensitizers, 6) Na_2[Cu(EDTA)].

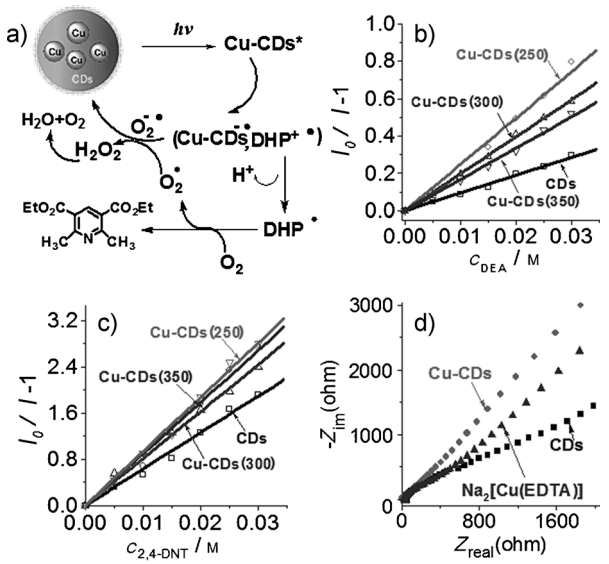

Figure 4. a) Mechanism for the photooxidation of 1,4-DHP with Cu-CDs. Stern–Volmer plot of the emission intensity of CDs and Cu-CDs with various amounts of b) DEA and c) 2,4-dinitrotoluene (DNT) upon excitation at $\lambda=350$ nm in H_2O. d) Nyquist diagrams for EIS measurements of Cu-CDs(●), Na_2[Cu(EDTA)] (▲), and CDs(■).

product was further demonstrated by monitoring changes in the UV/Vis absorption spectra, the ^{1}H NMR spectra, and in the HRMS (Figure S10, 11). After irradiation of the solution of 1,4-DHP alone or the solution of 1,4-DHP with Na_2[Cu(EDTA)] for 160 min, there is no obvious decrease of the absorption at $\lambda=374$ nm, indicating no conversion of 1,4-DHP. For pure CDs as the photocatalyst, the yield of **1b** only reached 17.4%. As the content of Cu dopant in Cu-CDs increased, the formation of product **1b** improved. For example, the yield of **1b** catalyzed by Cu-CDs(250) (Cu content = 2.1%) come to 60.8%, which is 3.5 times higher than that of CDs.

The photooxidation velocities of Cu-CDs as the photocatalysts were studied by plotting the $\ln(A_t/A_0)-t$ curves, as shown in Figure S9 and Table S1. The slope (k_{obs}) of the photooxidation with Cu-CDs(250) is 46×10^{-3} min^{-1}, which is higher than those of Cu-CDs prepared at 300 °C (Cu-CDs-(300); 43×10^{-3} min^{-1}) and at 350 °C (Cu-CDs(350); 26×10^{-3} min^{-1}). These results indicate that the actual photocatalysts are Cu-CDs, but not Na_2[Cu(EDTA)], and that the incorporated Cu–N dopants have enhanced the photocatalytic ability of the CDs.

Electron transfer is a crucial underlying process for the photooxidation reaction. The mechanism, involving electron transfer for the photooxidative aromatization of 1,4-DHP catalyzed by Cu-CDs, is proposed in Figure 4a, wherein the role of Cu-CDs changes from being an electron acceptor to an electron donor. First, Cu-CDs were photoexcited into the excited state (Cu-CDs*) and subsequent electron transfer from 1,4-DHP (electron donor) to Cu-CDs* (electron acceptor) produced the Cu-CD radical (Cu-CDs$^{\bullet-}$) and the 1,4-DHP radical cation (1,4-DHP$^{\bullet+}$). Highly reactive 1,4-DHP$^{\bullet+}$ is preferable to release H^+ (1,4-DHP$^{\bullet}$), and electron transfer process from 1,4-DHP$^{\bullet}$ to O_2 results in the production of the final aromatization product **1b** and the reactive oxygen radical $O_2^{\bullet}$. Subsequently, $O_2^{\bullet}$ gains an electron from Cu-CDs$^{\bullet-}$ (electron donor), which leads to the recovery of the photocatalyst, producing concomitantly the superoxide anion radical ($O_2^{\bullet-}$). Finally, $O_2^{\bullet-}$ reacts with H^+ to produce H_2O_2. As a result of the presence of CDs, H_2O_2 is subsequently decomposed into O_2 and H_2O, meeting the demands of green chemistry by producing environmentally friendly side products.[16,37]

To confirm the electron-transfer mechanism, ESR spectroscopy was employed to monitor the trapping of $O_2^{\bullet-}$ intermediates with 5,5-dimethyl-1-pyrroline-*N*-oxide (DMPO), which acts as a scavenger for $O_2^{\bullet-}$ as shown in Figure S12. 1,4-DHP, Cu-CDs, and DMPO were mixed in an aerated aqueous solution. A strong signal for the DMPO–$O_2^{\bullet-}$ adduct was detected. In the absence of any of the three reagents, no signal was detected. Compared with that of pure CDs, Cu-CDs show a stronger signal for the DMPO–$O_2^{\bullet-}$ adduct, indicating that Cu–N dopants have improved the efficiency of electron transfer from the substrate to the Cu-CDs, as well as from the Cu-CDs to O_2.

For an efficient electron-transfer process, excellent electron accepting and donating abilities and strong conductivity are key. Herein, these three factors are examined for Cu-CDs. First, the quenching effect of emission intensity by the known electron acceptor 2,4-dinitrotoluene (DNT, −0.9 V vs. NHE) and electron donor *N*,*N*-diethylaniline (DEA, 0.88 V vs. NHE) were measured to study the electron accepting and donating abilities of Cu-CDs as shown in Figure S11.[4,38] The Stern–Volmer plots, in which the integrated emission intensity was plotted versus the quencher concentration, assisted in analyzing the emission quenching in Figure 4.

When adding with different concentration of DEA, the emission intensity was quenched to a different extent with different concentrations of DEA (Figure S13). The Stern–

Volmer quenching constants (K_{SV}) for Cu-CDs(250), Cu-CDs(300), Cu-CDs(350), and CDs are 24.78 M^{-1}, 19.8 M^{-1}, 16.77 M^{-1}, and 9.54 M^{-1}, respectively (Figure 4b).[38] With increasing Cu content, the electron-accepting abilities of Cu-CDs were enhanced. Cu-CDs also acted as a strong electron donor, allowing highly efficient emission quenching by 2,4-dinitrotoluene (Figure S14). The K_{SV} value of Cu-CDs incorporating Cu–N dopants is about 95 M^{-1}, which is higher than that of CDs (65.7 M^{-1}; Figure 4c). The above results confirmed that introducing Cu–N into CDs could enhance the electron donating and accepting abilities, which are beneficial to their application in photooxidation reactions.

Furthermore, the conductivities of the Cu-CDs were measured using a DDS-307A electric conductivity meter. The electric conductivity of the Cu-CDs(250), Cu-CDs(300), and Cu-CDs(350) are 171.8 $\mu S\,cm^{-1}$, 113.9 $\mu S\,cm^{-1}$, and 104.4 $\mu S\,cm^{-1}$, respectively (Table S1). Additionally, Nyquist diagrams for electrochemical impedance spectroscopy (EIS) measurements of Cu-CDs, Na_2[Cu(EDTA)], and pure CDs were studied (Figure 4d). The diameter of the semicircle of these complexes in the Nyquist plots close to zero suggests an ultra-small interface electron resistance ($R_{ct} \approx 0$).[39,40] At the same time, the slope of the Nyquist plots of Cu-CDs is higher than others, indicating that Cu-CDs have higher electron diffusion ability.[41] Therefore, it is clear that Cu–N dopants have enhanced the conductivity of CDs, which would also benefit the efficiency of electron transfer in the photooxidation reaction.

In conclusion, Cu–N-doped CDs were successfully synthesized by a facile one-step pyrolysis from Na_2[Cu(EDTA)], wherein Cu-CDs prepared at 250 °C shows the highest Cu content of 2.1 %. Under an atmosphere of air, Cu-CDs were used as photocatalysts for the photooxidation of 1,4-DHP in aqueous solution. In this reaction, the yield of the product is 60.80 %, which is 3.5 times higher than that measured when pure CDs were employed. Based on the emission quenching and conductivity measurements, Cu–N dopants were found to enhance the electron-accepting and electron-donating abilities as well as the conductivity of CDs. These improved properties ultimately benefit the entire electron-transfer process and further improve the photocatalytic ability.

Experimental Section

Synthesis and purification of Cu-CDs and CDs: A quartz boat filled with Na_2[Cu(EDTA)] (analytical reagent, 1.6 g) was placed in the center of a quartz tube and calcined in a tube furnace at 250 °C, 300 °C, or 350 °C for 2 h at a heating rate of 5 °C min^{-1} under a N_2 atmosphere (Figure 1a). The product was ground and dissolved in water (100 mL), and the suspension was ultrasonically treated (300 W, (40 kHz) for 15 min at room temperature, and then centrifuged at a high speed (10000 rpm) for 20 min. The upper brown solution was filtered using a slow-speed quantitative millipore filter (0.25 μm) to remove the nonfluorescent deposited Na salts. After the filtration process, the solution was dialyzed with a MD34 (3500 Da) dialysis tube for 48 h to remove the remaining salts and small fragments. Pure luminescent Cu-CDs powder was obtained by drying the concentrated solution at 60 °C for 24 h. The powder is soluble in water and some organic polar solvents.

Keywords: carbon dots · doping · electron transfer · luminescence · photooxidation

How to cite: *Angew. Chem. Int. Ed.* **2015**, *54*, 6540–6544
Angew. Chem. **2015**, *127*, 6640–6644

[1] a) B. König in *Chemical Photocatalysis*, *Vol. 7,8* (Eds.: F. Telý, O. Reiser, G. Kachkovskyi, V. Kais, P. Kohls, S. Paria, M. Pirtsch, D. Rackl, H. Seo), Wiley-VCH, Weinheim, **2013**, pp. 111–149; b) Y. Yamada, T. Miyahigashi, H. Kotani, K. Ohkubo, S. Fukuzumi, *J. Am. Chem. Soc.* **2011**, *133*, 16136; c) A. T. Bell, *Science* **2003**, 299, 1688.
[2] C. Q. Ding, A. W. Zhu, Y. Tian, *Acc. Chem. Res.* **2014**, *47*, 20.
[3] L. Cao, M. J. Meziani, S. Sahu, Y. P. Sun, *Acc. Chem. Res.* **2013**, *46*, 171.
[4] H. T. Li, Z. H. Kang, Y. Liu, S. T. Lee, *J. Mater. Chem.* **2012**, *22*, 24230.
[5] X. M. Li, S. L. Zhang, S. A. Kulinich, Y. L. Liu, H. B. Zeng, *Sci. Rep.* **2014**, *4*, 4976.
[6] a) Q. Liu, B. D. Guo, Z. Y. Rao, B. H. Zhang, J. R. Gong, *Nano. Lett.* **2013**, *13*, 2436; b) M. Wu, Y. Wang, W. Wu, C. Hu, X. Wang, J. Zheng, Z. Li, B. Jiang, J. Qiu, *Carbon* **2014**, *78*, 480.
[7] H. T. Li, R. H. Liu, Y. Liu, H. Huang, H. Yu, H. Ming, S. Y. Lian, S. T. Lee, Z. H. Kang, *J. Mater. Chem.* **2012**, *22*, 17470.
[8] X. Zhang, F. Wang, H. Huang, H. T. Li, X. Han, Y. Liu, Z. H. Kang, *Nanoscale* **2013**, *5*, 2274.
[9] W. T. Wu, L. Y. Zhan, K. Ohkubo, Y. Yamada, M. B. Wu, S. Fukuzumi, *J. Photochem. Photobiol. B* **2014**, DOI: 10.1016/j.jphotobiol.2014. 10.018.
[10] F. Wang, M. Kreiter, B. He, S. P. Pang, C. Y. Liu, *Chem. Commun.* **2010**, *46*, 3309.
[11] S. Chandra, P. Patra, S. H. Pathan, S. Roy, S. Mitra, A. Layek, R. Bhar, P. Pramanik, A. Goswami, *J. Mater. Chem. B* **2013**, *1*, 2375.
[12] X. M. Li, Y. L. Liu, X. F. Song, H. Wang, H. S. Gu, H. B. Zeng, *Angew. Chem. Int. Ed.* **2015**, *54*, 1759; *Angew. Chem.* **2015**, *127*, 1779.
[13] J. Ge, M. Lan, B. Zhou, W. Liu, L. Guo, H. Wang, Q. Jia, G. Niu, X. Huang, H. Zhou, X. Meng, P. Wang, C. Lee, W. Zhang, X. Han, *Nat. Commun.* **2014**, *5*, 4596.
[14] R. H. Liu, H. Huang, H. T. Li, Y. Liu, J. Zhong, Y. Y. Li, S. Zhang, Z. H. Kang, *ACS Catal.* **2014**, *4*, 328.
[15] N. Y. Liu, J. Liu, W. Q. Kong, H. Li, H. Huang, Y. Liu, Z. H. Kang, *J. Mater. Chem. B* **2014**, *2*, 5768.
[16] a) J. Liu, H. C. Zhang, D. Tang, X. Zhang, L. K. Yan, Y. Z. Han, H. Huang, Y. Liu, Z. H. Kang, *ChemCatChem* **2014**, *6*, 2634; b) J. Liu, Y. Liu, N. Liu, Y. Han, X. Zhang, H. Huang, Y. Lifshitz, S.-T. Lee, J. Zhong, Z. Kang, *Science* **2015**, *347*, 6225.
[17] J. Q. Pan, Y. Z. Sheng, J. X. Zhang, J. M. Wei, P. Huang, X. Zhang, B. X. Feng, *J. Mater. Chem. A* **2014**, *2*, 18082.
[18] H. Ming, Z. Ma, Y. Liu, K. M. Pan, H. Yu, F. Wang, Z. H. Kang, *Dalton Trans.* **2012**, *41*, 9526.
[19] Y. Guo, B. X. Li, *Carbon* **2015**, *82*, 459.
[20] a) R. G. Reddy, S. Balasubramanian, K. Chennakesavulu, *J. Mater. Chem. A* **2014**, *2*, 15598; b) C. Balzani, S. Campagna in *Topics in Current Chemistry*, *Vol. 280* (Eds.: N. Armaroli, G. Accorsi, F. Cardinali, A. Listorti), Springer, Berlin, **2007**, pp. 70–110.
[21] A. Poater, M. Sola, *Beilstein J. Org. Chem.* **2013**, *9*, 585.
[22] K. D. Karlin, S. Kaderli, A. Zuberbuhler, *Acc. Chem. Res.* **1997**, *30*, 139.
[23] V. S. I. Sprakel, M. C. Feiters, W. M. Klaucke, M. Klopstra, J. Brinksma, B. L. Feringa, K. D. Karlin, R. J. M. Nolte, *Dalton Trans.* **2005**, 3522.
[24] D. Zhang, L. Wu, L. Zhou, X. Han, Q. Yang, L. Zhang, C. Tung, *J. Am. Chem. Soc.* **2004**, *126*, 3440.
[25] G. Merza, B. László, A. Oszkó, G. Pótári, K. Baán, A. Erdőhelyi, *J. Mol. Catal. A* **2014**, *393*, 117.

[26] J. L. Yang, X. P. Shen, Z. Y. Ji, H. Zhou, G. X. Zhu, K. M. Chen, *Appl. Surf. Sci.* **2014**, *316*, 575.
[27] Z. H. Kang, E. B. Wang, B. D. Mao, Z. M. Su, L. Gao, S. Y. Lian, L. Xu, *J. Am. Chem. Soc.* **2005**, *127*, 6534.
[28] N. Liu, F. Luo, H. X. Wu, Y. H. Liu, C. Zhang, J. Chen, *Adv. Funct. Mater.* **2008**, *18*, 1518.
[29] J. Lu, J. X. Yang, J. Z. Wang, A. Lim, S. Wang, K. P. Loh, *ACS Nano* **2009**, *3*, 2367.
[30] Z. T. Luo, Y. Lu, L. A. Somers, A. T. C. Johnson, *J. Am. Chem. Soc.* **2009**, *131*, 898.
[31] G. Eda, Y. Y. Lin, C. Mattevi, H. Yamaguchi, H. A. Chen, I. S. Chen, C. W. Chen, M. Chhowalla, *Adv. Mater.* **2010**, *22*, 505.
[32] M. Röckert, M. Franke, Q. Tariq, S. Ditze, M. Stark, P. Uffinger, D. Wechsler, U. Singh, J. Xiao, H. Marbach, H. P. Steinrück, O. Lytken, *Chem. Eur. J.* **2014**, *20*, 8948.
[33] J. J. Brege, C. E. Hamilton, C. A. Crouse, A. R. Barron, *Nano Lett.* **2009**, *9*, 2239.
[34] P. Gayathri, K. A. Senthil, *Langmuir* **2014**, *30*, 10513.
[35] T. A. Mohamed, I. A. Shaaban, R. S. Farag, W. M. Zoghaib, M. S. Afifi, *Spectrochim. Acta Part A* **2015**, *135*, 417.
[36] J. Xia, S. Yuan, Z. Wang, S. Kirklin, B. Dorney, D. J. Liu, L. Yu, *Macromolecules* **2010**, *43*, 3325.
[37] F. Y. Chen, X. Zhao, H. J. Liu, J. H. Qu, *Appl. Catal. B* **2014**, *158*, 85.
[38] X. Wang, L. Cao, F. S. Lu, M. J. Meziani, H. T. Li, G. Qi, B. Zhou, B. A. Harruff, F. Kermarreca, Y. P. Sun, *Chem. Commun.* **2009**, 3774.
[39] Z. T. Li, G. L. Wu, D. Liu, W. T. Wu, B. Jiang, J. T. Zheng, Y. P. Li, J. H. Li, M. B. Wu, *J. Mater. Chem. A* **2014**, *2*, 7471.
[40] X. B. Lu, X. Wang, J. Jin, Q. Zhang, J. P. Chen, *Biosens. Bioelectron.* **2014**, *62*, 134.
[41] J. J. Feng, G. Zhao, J. J. Xu, H. Y. Chen, *Anal. Biochem.* **2005**, *342*, 280.

Received: February 27, 2015
Published online: April 16, 2015

